Main Lobe Interference Suppression Method Based on Fractional Fourier Transform

Jian Yang, Yuwei Tu, Jian Lu, Fengtao Xue, and Zhi Geng

Abstract The Fractional Fourier transform has a good energy aggregation effect for linear frequency modulation (LFM) signals commonly used in radar systems. Therefore, this paper proposes a mainlobe interference suppression method based on Fractional Fourier transform (FRFT). Firstly, the mixed radar echo signal containing main lobe interference is processed by FRFT transform with specific LFM signal characteristics, then the interference and most noise energy are removed by filtering in the FRFT domain. Finally, FRFT inverse transformation recovers the target signal. Simulation verifies the effectiveness of the algorithm.

Keywords Anti-mainlobe interference · Fractional Fourier transform · FRFT domain filtering · Pulse compression

1 Introduction

The anti-jamming performance of radar is increasingly important in modern electronic warfare. Mainlobe interference reduces the output SINR of radar, increases false alarm rate, and makes it difficult for previous interference suppression algorithms against sidelobe interference to suppress mainlobe interference, which may cause mainlobe distortion and suppression of desired signals as interference. As one of the important means of electronic jamming, mainlobe interference can easily

J. Yang (✉) · Y. Tu
Xi'an Research Institute of Hi-Tech, Hongqing Town, Xi'an 710025, China
e-mail: yangjian@nudt.edu.cn

J. Lu
96921 Troops of the Chinese People's Liberation Army, Beijing 100001, China

F. Xue
Beijing Remote Sensing Equipment Research Institute, Beijing 100854, China

Z. Geng
Logistics Information Center, Former Joint Logistics Department of Chengdu Command, Chengdu 610015, China

W. Wang et al. (eds.), *Communications, Signal Processing, and Systems*, Lecture Notes in Electrical Engineering 1032, https://doi.org/10.1007/978-981-99-7505-1_8

deceive target distance, velocity, angle and other parameters, seriously affecting the normal operation and detection performance of radar system. In paper [1], a mainlobe interference suppression method based on low sidelobe constraint blocking matrix preprocessing (BMP) is proposed. The Angle of mainlobe interference is estimated using the singular value decomposition (SVD) method, and a blocking matrix is constructed to suppress mainlobe interference. In paper [2], the main lobe interference suppression technique of wideband noise based on space–time adaptive processing (STAP) is studied. A mainlobe interference suppression method based on oblique projection of eigenvalues is proposed in [3]. The eigenvalue oblique projection preprocessing matrix is constructed to filter out the main lobe interference, and then the influence of covariance mismatch matrix is reduced by diagonal loading. In [4], a four-channel monopulse technique for suppressing mainlobe interference was proposed. In Ref. [5], a method for anti-deception interference of an array radar was proposed. The idea based on FRFT transformation mentioned in the paper was applied to suppress the main lobe interference proposed in this paper. We propose a FRFT-based radar's primary lobe jamming suppression technique that uses FRFT transformation's special feature for linear frequency modulation signal. The algorithm can effectively suppress jamming and improve peak signal-to-noise ratio after pulse compression according to theoretical analysis. The performance of the proposed method is verified through comprehensive performance analyses and simulation results.

1.1 Signal Model

Using a linear frequency modulation signal as the transmission signal for a radar system, its mathematical expression in the time domain is (Fig. 1):

$$s(t) = \mathrm{rect}(t \Big/ T_p)\mathrm{e}^{\mathrm{j}2\pi f_c + \mathrm{j}\pi\kappa t^2} \tag{1}$$

In the formula, $s(t)$ is the radar transmission signal, $\mathrm{rect}(t \Big/ T_p)$ represents the rectangular pulse function, T_p represents the pulse width, f_c represents the signal carrier frequency, and κ represents the modulation frequency.

The mathematical model of the target in the radar echo needs to consider the time delay and frequency shift caused by the target distance and movement, then the mathematical model of the target echo signal is:

$$s_1(t) = s_0(t - \tau_1)\mathrm{e}^{-\mathrm{j}2\pi f_c \frac{2v_{r1}}{c}t} \tag{2}$$

In the formula, $s_1(t)$ is the echo signal of the target, τ_1 is the time delay of the echo signal. Because there is a distance between the radar and the target, there will be a time delay between the echo signal and the radar transmitted signal. The relationship between the time delay τ_1 of the target and the distance r_1 of the target is $\tau_1 = \frac{2r_1}{c}$.

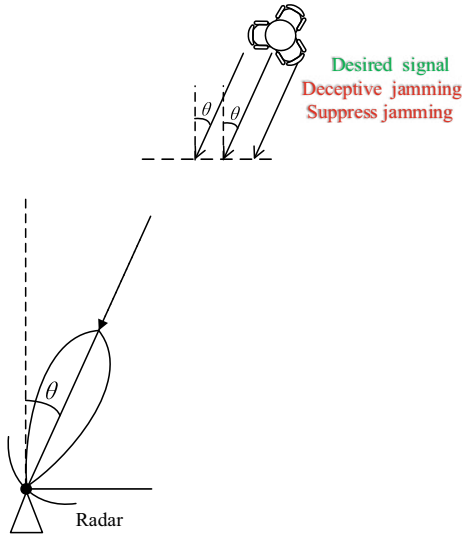

Fig. 1 Radar antenna signal reception schematic diagram

1.2 Principles Related to FRFT

In 1980, Namias first proposed the definition of Fractional Fourier transform from a purely mathematical perspective in terms of eigenvalues and eigenfunctions [6]. Subsequently, McBride provided a more rigorous mathematical definition for Fractional Fourier transform in integral form [7]. Below we give the basic definition of Fractional Fourier transform from the perspective of integral transformation.

The p-th order Fractional Fourier transform of a time-domain signal x(t) defined in the t-domain is a linear integral operation:

$$F^p(u) = \int_{-\infty}^{+\infty} K_p(u,t)x(t)dt \tag{3}$$

In the formula, $K_p(u,t)$ is the kernel function of FRFT, and p represents the transformation order, which can be specifically written as

$$K_p(t,u) = \begin{cases} \sqrt{(1-j\cot\alpha)/(2\pi)}\exp\left(j\frac{u^2+t^2}{2}\cot\alpha - jut\csc\alpha\right), & \alpha \neq n\pi \\ \delta(t-u), & \alpha = 2n\pi \\ \delta(t+u), & \alpha = (2n+1)\pi \end{cases} \tag{4}$$

After variable substitution $u = u/\sqrt{2\pi}$ and $t = t/\sqrt{2\pi}$, Formula (3) can be further written as

$$F^p(u) = \{ F^p[x(t)](u)\} = \int_{-\infty}^{+\infty} K_p(u,t)x(t)dt, \quad 0 < |p| < 2, 0 < |\alpha| < 2$$

$$= \begin{cases} {}_\alpha \exp(j\frac{u^2+t^2}{2}\cot\alpha - jut\csc\alpha)x(t)dt, & \alpha \neq n\pi \\ x(t), & \alpha = 2n\pi \\ x(-t), & \alpha = (2n+1)\pi \end{cases} \tag{5}$$

where $A_\alpha = \sqrt{(1 - j\cot\alpha)/(2\pi)}$, the definition of FRFT given by formula (5) is linear but not shift-invariant (except for $p = 4n$), because the kernel function is not only a function of (u, t) but also a function of p. It is worth noting that F^{4n} and F^{4n+2} are equivalent to the identity operator I and parity operator P respectively. For $p = 1, \alpha = \pi/2, A_\alpha = 1$, and:

$$F^1(u) = \int_{-\infty}^{+\infty} \exp(j2\pi ut)x(t)dt \tag{6}$$

It can be seen that $F^1(u)$ is the ordinary Fourier transform of $x(t)$, and similarly, $F^{-1}(u)$ is the ordinary inverse Fourier transform of $x(t)$.

Linear frequency modulation signals are typical non-stationary signals with large time-bandwidth products, widely used in radar, communication, sonar detection and other fields, especially in radar systems. As a linear transform that decomposes signals into chirp bases without cross-term interference, Fractional Fourier transform is particularly suitable for processing chirp-like signals. Analogous to how any vector on a two-dimensional plane can be decomposed into two basis vectors along x and y axes, any LFM signal can also be decomposed into two chirp bases. By choosing an appropriate order p, FRFT can concentrate the energy of the chirp signal on the basis vector along this direction, forming an impulse pulse, whereas conventional Fourier transform usually does not align with this "optimal direction", resulting in more dispersed energy with a certain bandwidth. Therefore, FRFT has good energy aggregation characteristics for LFM signals in some fractional transform domains [8].

2 Mainlobe Interference Suppression Algorithm

Assume that the time-domain representation of an arbitrary LFM signal is expressed as $\phi(t) = \exp(\mathrm{j}2\pi f_0 t + \mathrm{j}\pi\kappa t^2)$. Then, the p th order FRFT transform of LFM signal can be written as [9]:

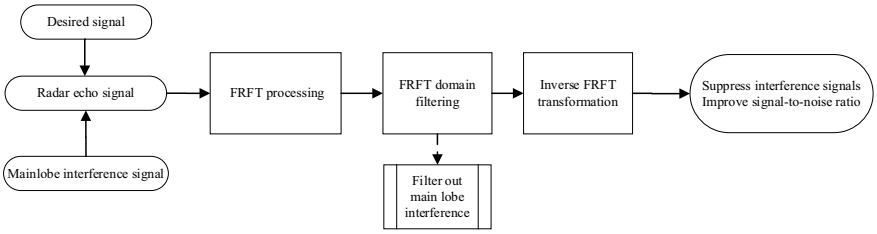

Fig. 2 Flowchart of main lobe interference suppression algorithm based on FRFT

$$F^p[x_{LFM}(t)](u) = F^p[\phi(t)](u)$$
$$= \begin{cases} \sqrt{\frac{1+\mathrm{j}\tan\alpha}{1+\kappa\tan\alpha}}\exp\left[\mathrm{j}\pi\frac{(\kappa-\tan\alpha)u^2+2uf_c\sec\alpha-f_c^2\tan\alpha}{1+\kappa\tan\alpha}\right], & \alpha-\arctan\kappa\neq(2i+1)\pi/2 \\ \sqrt{\frac{1}{1-\mathrm{j}\kappa}}\exp[\mathrm{j}\pi\cos\alpha(-f_c^2\sin\alpha+2uf_c)]\delta(u-f_c\sin\alpha), & \alpha-\arctan\kappa=(2i+1)\pi/2 \end{cases} \tag{7}$$

Utilizing the characteristic of linear frequency modulation signals in Fractional Fourier transform, we propose a radar mainlobe interference suppression technique based on FRFT. The received mainlobe interference mixed echo signal is first processed by FRFT, followed by filtering in the FRFT domain to remove most of the suppressed interference and noise energy. The target signal is then recovered by inverse FRFT. Theoretical analysis suggests that this algorithm can effectively suppress interference and significantly improve the peak signal-to-noise ratio after pulse compression. By analyzing the phase relationship between peak values of continuous pulse echoes and improving the signal-to-noise ratio of fractional domain echo signals through coherent accumulation, it is possible to extract peak values of LFM signals under low signal-to-noise ratio conditions. The design method process is shown in the Fig. 2.

Since both deceptive interference signals and target echoes are wideband LFM signals with the same modulation rate κ, for ease of analysis, we first analyze the phase relationship in the fractional domain of the target echo signals received by radar antenna after p_0 th order FRFT processing. It can be derived that by representing the target echo component in the m-th echo received by the radar antenna as a phase-shifted and frequency-shifted form of an LFM signal.

$$s_0(t_m,\tilde{t}) = \chi_m\gamma(m)\exp(-\mathrm{j}2\pi f_m\tilde{t}+\mathrm{j}\pi\kappa\tilde{t}^2) \tag{8}$$

where,

$$\chi_m = \mathrm{rect}\left[\frac{\tilde{t}-\tau(t_m)}{T_p}\right], \quad f_m = \kappa\tau(t_m)$$
$$\gamma(m) = \exp\{\mathrm{j}2\pi f_c[-\tau(t_m)]+\mathrm{j}\pi\kappa[\tau(t_m)]^2\} \tag{9}$$

The above equation can be regarded as the result of an LFM signal with a carrier frequency of f_m and a modulation rate of κ undergoing data truncation and linear transformation. In the actual digital sampling process, the radar antenna uses the same distance gate for digitizing samples of the same echo.

According to the aforementioned analysis, FRFT has many excellent properties such as reversibility, linearity, exponential additivity, commutativity, associativity, time-shift property and frequency-shift property [7–10]. Utilizing these properties, we analyze the phase relationship in fractional domain of target echo signals received by radar antenna. Since $\tan\alpha_0 = \kappa \gg 1$, then $\kappa\cos\alpha_0 = \sin\alpha_0 \approx 1$. According to Eqs. (7) and (8), the fractional domain form $F^{p_0}[\breve{s}_0(t_m, \tilde{t})](u)$ can be further expressed as:

$$\begin{aligned} &F^{p_0}[\breve{s}_0(t_m, \tilde{t})](u) \\ &= A_\kappa \gamma(m) \exp\left\{-\mathrm{j}\pi \frac{\kappa^3}{\kappa^2+1}[\tau(t_m)]^2\right\} \cdot \exp(-\mathrm{j}2\pi f_m \cos\alpha_0 u) \\ &\approx A_\kappa \gamma(m) \exp\left\{-\mathrm{j}\pi \frac{\kappa^3}{\kappa^2+1}[\tau(t_m)]^2\right\} \cdot \exp\{-\mathrm{j}2\pi[\tau(t_m)]u\} \\ &\approx A_\kappa \gamma(m) \exp\{-\mathrm{j}\pi\kappa[\tau(t_m)]^2\} \cdot \exp\{-\mathrm{j}2\pi[\tau(t_m)]u\} \\ &= A_\kappa \exp\{-\mathrm{j}2\pi f_c[\tau(t_m)\} \cdot \exp\{-\mathrm{j}2\pi[\tau(t_m)]u\} \end{aligned} \tag{10}$$

wherein, the transformation order p_0 is a specific transformation order that converts an LFM signal into a complex single-frequency point signal in a fractional Fourier domain. That is, after performing FRFT with an order of p_0, the LFM signal becomes a sine wave with a frequency of $f = f_0 \cos\alpha_0$ [9]. In digital processing, its specific transformation order is expressed as: $p_0 = \frac{2}{\pi}\arctan\left(\frac{N_g\kappa}{f_s^2}\right)$.

Since discrete FRFT operations also require dimension normalization processing, this paper adopts discrete scaling proposed in literature to perform scale transformation[11]. By decomposing the above equation according to the radar antenna received signal model, we obtain the fractional domain data $\mathbf{S}_m(u)$ obtained by processing the target signal of sampling mth echo with p_0-order FRFT as follows:

$$\mathbf{s}_m(u) = A_\kappa \exp[-\mathrm{j}2\pi\tau(t_m)(f_c+u)] = A_\kappa \exp[-\mathrm{j}2\pi f_c\tau(t_m) - \mathrm{j}2\pi\tau(t_m)u)] \tag{11}$$

From Eq. (11), it can be seen that the incident signal of the m-th echo received by the radar is equivalent to the fractional domain signal $\mathbf{s}_m(u)$, and the fractional domain frequency of signal $\mathbf{s}_m(u)$ is determined by time delay $\tau(t_m)$. According to the dimension normalization method in literature [11], the fractional domain frequency corresponding to signal $\mathbf{s}_m(u)$ can be expressed as:

$$f_{nu} = \left| \frac{\frac{\tau_{\max}+\tau_{\min}}{2} - \tau(t_m)}{\sqrt{\frac{\tau_{\max}-\tau_{\min}}{f_s}}} \right| \tag{12}$$

In the equation, $|\cdot|$ represents taking absolute value, $\tau_{\min}$ and $\tau_{\max}$ respectively represent the time delay corresponding to the minimum value $R_{\min}$ and maximum value $R_{\max}$ of distance gate. Since the frequency of target echo signal in fractional domain is determined by target's time delay relative to center of gate, prior information about target position is usually known before transmitting broadband signal. For example, it is known that target distance interval is $[r_{\min}, r_{\max}] \subset [R_{\min}, R_{\max}]$, and assuming that two distance intervals have a common center. Accordingly, the highest frequency of target echo in fractional domain is:

$$f_{mu} = \frac{\frac{\tau_{\max}+\tau_{\min}}{2} - \frac{2r_{min}}{c}}{\sqrt{\frac{\tau_{\max}-\tau_{\min}}{f_s}}} \tag{13}$$

Therefore, if the echo signal of the interference target is outside the distance interval $[r_{\min}, r_{\max}]$, the frequency of the interference signal in the fractional domain will be greater than f_{mu}, and the interference signal can be filtered out by a low-pass filter in the fractional domain.

3 Simulation Results

A desired signal and a noise suppression interference signal were set up along with two deception interference signals. All the signals are coming from the same direction. The velocities of interference signals 1 and 2 were set to − 10 m/s and − 15 m/s respectively, while the velocity of the desired signal was set to 15 m/s. The signal-to-noise ratio was set as 0 dB, and the interference noise ratio of two deceptive interferences and one suppressing interference was set as 18 dB,18 dB and 35 dB respectively (Fig. 3).

From the time–frequency diagrams before and after algorithm processing, it can be seen that the algorithm has clearly filtered out most of the interference in the frequency band after processing, especially suppressing interference.

By processing the echo signal and performing pulse compression and coherent processing, an R-D plane is obtained for moving target detection and parameter estimation. The algorithm simulation results are shown in the Fig. 4.

According to the simulation results, the proposed algorithm can significantly suppress main lobe interference from two signals in the same direction as the desired signal, thereby making the desired signal more prominent and significantly improving the signal-to-noise ratio.

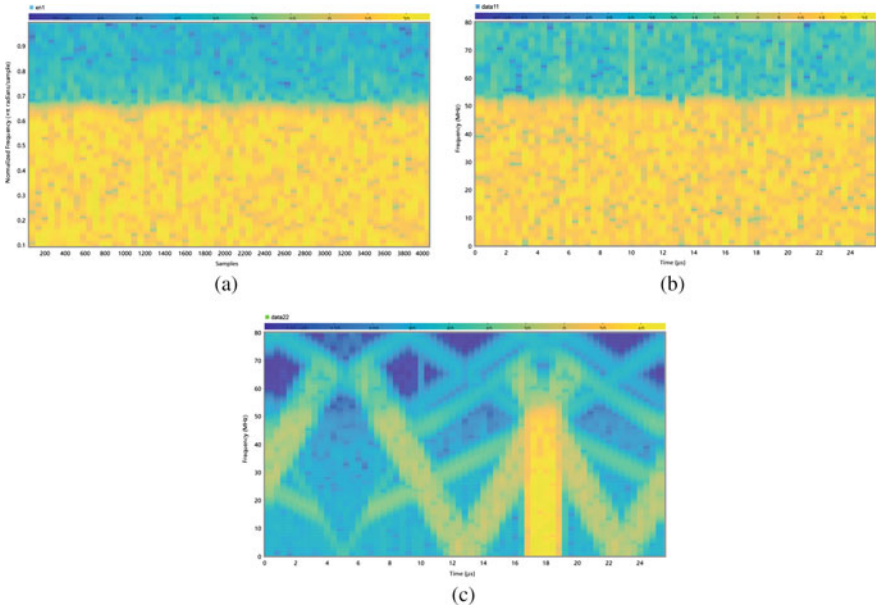

Fig. 3 The time–frequency diagram of the signal: **a** noise suppression interference signal time–frequency distribution diagram, **b** time–frequency distribution of transmitted signal, **c** time–frequency distribution of the signal after algorithm processing

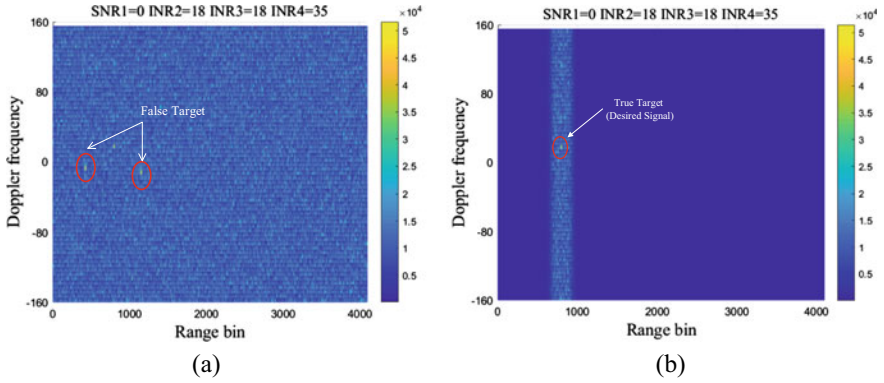

Fig. 4 **a** R-D distribution of simulated echo received signal **b** R-D distribution of signal after algorithm processing

4 Conclusions

In this paper, we propose an algorithm that involves FRFT processing of the received mixed echo signal with primary lobe jamming. Most of the energy of suppressed jamming and noise in FRFT domain is filtered out. Simulation experiments show that the algorithm can effectively improve the estimation accuracy under the condition of low signal-to-noise ratio with the presence of the main lobe interference. The algorithm can improve the peak signal-to-noise ratio after pulse compression and improve the detection performance of the pulse compression radar.

Acknowledgements This research was funded by National Natural Science Foundation of China, grant numbers 62071481 and 61501471.

References

1. Haoyu M, Xiaodong Q, Xingyu Z, Wolin L, Zhengyan Z, Xiaopeng Y (2022) Mainlobe interference suppression method based on blocking matrix preprocessing with low sidelobe constraint. In: 2022 Asia-Pacific signal and information processing association annual summit and conference (APSIPA ASC), Chiang Mai, Thailand, pp 2065–2070. https://doi.org/10.23919/APSIPAASC55919.2022.9980066
2. Liao Y, Wu X, Wang Y (2018) The main lobe interference suppression algorithm for wideband interference. In: 2018 14th IEEE International conference on signal processing (ICSP), Beijing, China, pp 148–152. https://doi.org/10.1109/ICSP.2018.8652409
3. Meng H, Yang X, Gao S, Yu Z (2022) Main lobe interference suppression method based on eigenvalue oblique projection. J Signal Process 38(2):439–444
4. Xu A, Zhao C, Xue J, Li L, Meng F (2019) Four-channel monopulse technique for main-lobe interference suppression. In: 2019 IEEE 8th Joint international information technology and artificial intelligence conference (ITAIC), Chongqing, China, pp 1354–1357. https://doi.org/10.1109/ITAIC.2019.8785875
5. Yang J, Lu J, Tu Y et al (2022) Spatial deception suppression for wideband linear frequency modulation signals based on fractional Fourier transform with robust adaptive beamforming. Digital Signal Process 126:103485
6. Namias V (1980) The fractional Fourier transform and its application in quantum mechanics. J Inst Math Appl 25(3):241–265
7. McBride AC, Kerr FH (1987) On Namias' fractional Fourier transforms. IMA J Appl Math 39(2):159–175
8. Cowell DM, Freear S (2010) Separation of overlapping linear frequency modulated (LFM) signals using the fractional Fourier transform. IEEE Trans Ultrason Ferroelectr Freq Control 57(10):2324–2333. https://doi.org/10.1109/TUFFC.2010.1693. PMID: 20889420
9. Ma Y, Wang R, Du J (2013) Amplitude characteristics of linear frequency modulation signal in FRFT domain. In: 2013 IEEE international conference on signal and image processing applications, pp 431–434. https://doi.org/10.1109/ICSIPA.2013.6708045
10. Ozaktas HM et al (1996) Digital computation of the fractional Fourier transform. IEEE Trans Signal Process 44(9):2141–2141
11. Zhao XH, Deng B, Tao R (2005) Dimensional normalization in the digital computation of the Fractional Fourier transform. Trans Beijing Inst Technol 25(4):360–364